JOURNAL OF APPLIED ELECTROCHEMISTRY **22** (1992) 852-858

Electrochemical behaviour of zirconium metal and its oxide film in LiOH and HF solutions

J.-Y. HUOT

Centre de Technologie Noranda, 240 Hymus, Pointe-Claire (QUE), Canada, H9R 1G5

Received 4 April 1989, revised 14 February 1992; accepted 14 February 1992

The electroformation and *in situ* characterization of ZrO_2 in 0.1 M LiOH at 25°C reveal an insulating behaviour equivalent to that observed in other alkaline and acid media. Etched zirconium is found to be covered by a 2.0 nm oxide film, while the growth rate of the anodic film in 0.1 M LiOH is $2.1\ \mathrm{nm\ V^{-1}}$ and the dielectric constant is $30/r$ (r being the roughness factor). Chemical dissolution of the anodic film after times of up to 2.5×10^4 s is very slow in 0.1 M LiOH and 1 M Hcl, whereas ZrO_2 dissolves rapidly in 0.05 M HF, as shown by the reciprocal capacitance C^{-1}, which is found to follow the empirical relation $C^{-1} = A - Bt^{1/2}$ where $B = 2\ \mathrm{nm\,s^{-1/2}}$ in 0.05 M HF.

1. Introduction

Zirconium Zr has recently been the subject of numerrous investigations, mainly because of the stability of its passive film toward corrosion and hydrogen embrittlement and its small cross-section for neutron absorption, which make it a suitable material for use as pressure tubes immersed in lithiated heavy water for nuclear fuels [1].

The electrochemical stability of zirconium, a valve metal, is attributed to the stability and thickness of the ZrO_2 film covering the unstable bare metal [2]. In aqueous solutions, the standard potential at 20°C for Reaction 1 is -1.43 V/RHE:

$$ZrO_2 + 4H^+ + 4e^- \longrightarrow Zr + 2H_2O \qquad (1)$$

Thus the bare metal is always covered by an oxide film. The characterstics of ZrO_2^2 films on Zr depend strongly on the formation conditions [3]: that is, oxidation in O_2 at 550°C for thick films of 1–4 μm and anodic treatment in aqueous solutions near 25°C for thin films of 20–40 μm. The nature of the electrolyte is reported to influence the formation of a porous anodic oxide film in that it affects the ionic transport in the film without substantially modifying the physical properties of the oxide [4–6] or the stability and pitting attack of the film [2, 7]. This influence of the electrolyte could be due to the oxide being contaminated by incorporation of the electrolyte ions during anodic formation [6].

The electrochemical growth of anodic thin films on zirconium as a function of the surface preparation, electrode potential and pH reveals that the growth rate is not very pH-dependent for thicknesses of 10–30 μm [8], but ion incorporation becomes less favoured at high pH's [9]. The passive current at low anodic potentials is found to be independent both of the potential and the pH [10].

The kinetics of the dissolution of anodically formed ZrO_2 films have been investigated in HCl [11] and H_2SO_4 [12] using impedance and potential measurements and were found to be a function of the acid concentration, the temperature and the formation voltage of the oxide film.

The present study concerns anodic film formation and electrochemical characterization in 0.1 M LiOH solutions at 25°C followed by dissolution of the anodically formed oxide film in 1 M HCl and 0.05 M HF solutions.

2. Experimental details

Thermostated glass cells were used for the electrochemical measurements. The three-electrode system was controlled by a Solartron 1286 potentiostat and the impedance measurements were performed with a Solartron 1250 Frequency Analyzer.

The aqueous solutions were 1 M HCl, 0.05 M HF and 0.1 M LiOH (Fisher) solutions. No other species were dissolved. All solutions were deaerated with nitrogen prior to the electrochemical experiments.

The working electrodes were 3.2 cm (area $1.0\ \mathrm{cm^2}$) polycrystalline zirconium wires (99.8%, AESAR, 1.0 mm dia.) sealed in glass. The counterelectrode was a platinum foil of $15\ \mathrm{cm^2}$. A saturated calomel electrode (SCE) was used as the reference electrode; its measured potential was 0.257, 0.965, and 0.388 V with respect to the reversible hydrogen electrode in 1 M HCl, 0.1 M LiOH and 0.05 M HF, respectively.

Two different methods of surface preparation were used: mechanical polishing and etching.

(i) *Mechanical polishing*. The specimens were abraded with emery paper (600) then polished with wet alumina powder (0.3 μm) until a smooth grey surface was obtained.

(ii) *Etching*. After soft mechanical polishing, the specimens were immersed in a solution of 1 : 4 : 5 parts by volume 48% HF, 98% HNO_3 and triple-distilled water and carefully rinsed. The immersion period was stopped a few seconds after the distinctly visible hydrogen evolution; typical time of etching was 5–10 s.

Thin oxide films on zirconium were produced and

0021-891X/92 © 1992 Chapman & Hall

investigated in an alkaline solution as a function of the metal surface preparation and the anodic potential at 25°C by simultaneously measuring the current (sweep rate $50\,mV\,s^{-1}$) and the electrode capacitance (1000 Hz, 5 mV) during a single cycle of voltage between 0 and $12\,V_{RHE}$. Dissolution of the anodically formed ZrO_2 was investigated by simultaneously measuring the open-circuit potential and the electrode capacitance (1000 Hz. 5 mV) in various media as a function of time.

3. Results and discussion

3.1. *Electroformation and characterization of* ZrO_2 *in* 0.1 M LiOH

An idea of the frequence response of the Zr/ZrO_2 system in 0.1 M LiOH is obtained from a.c. impedance diagrams in the high frequency range. After etching, the zirconium electode polarized at $-1.25\,V_{SCE}$ ($-0.28\,V_{RHE}$) in 0.1 M LiOH yields a simple diagram (Fig. 1a) which is tentatively described in terms of a resistance R and capacitance C in series. According to the Equation 2, the ideal response for such a RC system should be a vertical line in the Nyquist plot.

$$Z = R - \frac{j}{\omega C} \tag{2}$$

The actual dependence of C and R on frequency (Fig. 1b) suggests that the $Zr/ZrO_2/LiOH$ system does not behave as an ideal capacitor connected in series with the resistance of the solution. This is a somewhat complex system where the frequency-dependencies were already attributed to a distribution of dielectric relaxation times within the zirconium [9] or titanium [13] oxide. An equivalent impedance diagram was obtained at +5.5 V, revealing an equivalent behaviour for zirconium over a wide range of anodic potentials and suggesting that a residual oxide film remains on the zirconium electrode after etching. Although both the resistance and the capacitance are frequency dependent, it remains possible to evaluate relative oxide properties and to estimate some intrinsic properties. An alternative way would be to get impedance spectrum over several decades of frequencies and to fit the data [14].

A thin ZrO_2 film was grown on zirconium by means of a potentiodynamic experiment in the form of a single-cycle polarization starting with $50\,mV\,s^{-1}$ at -1.5 V. The capacitance values of the electrode are obtained by simultaneously measuring the impedance with a 1 kHz/5 mV signal superimposed on the d.c. potential and assuming that the oxide behaves as an ideal capacitor connected in series with the resistance of the solution. It was verified that this signal does not modify the anodic i–E trend.

The anodic current density in the positive scan was seen to reach an almost constant value of $0.4\,mA\,cm^{-2}$ for etched and mechanically polished zirconium wires (Fig. 2). The current plateau means that the electric field within the oxide film is constant under these conditions. In the case of polished wire, a small peak occurs at +2.5 V, at the beginning of the oxide formation, suggesting a contribution of side reactions such as oxygen evolution and metal dissolution. All the following analyses and experiments were therefore performed with etched zirconium wires. No bubbling on the electrode surface was visible at 12 V in 0.1 M LiOH.

During the positive scan, the electrode capacitance decreases continuously, reaching a low value of $\sim 1\,\mu F\,cm^{-2}$ beween 9 and 12 V whatever the electrode treatment prior to anodic oxidation. As already reported for thin oxide films [3], the electrode changes colour from grey to purple after anodic oxidation.

During the negative scan, the current density decreases at 10 V but the capacitance remains almost constant. This behaviour is typical of valve metals such as titanium [13] and zirconium [8], which are characterized by irreversible oxide growth during the positive scan and a constant thickness during the negative scan. This means that the capacitance is independent of the potential, as anticipated for the behaviour of an insulating material. Since ZrO_2 is a semiconductor, it becomes an insulator when the deep depletion layer of the space charge becomes equivalent to or larger than the thickness of the anodic film. For high anodic potentials, the anodic film should be insulating because of the absence of a chargeable space charge, while for low potentials the film should display a semiconductive behaviour because the deep depletion layer will vary with the potential.

The film-electrolyte interface is described by two capacitances in series:

$$\frac{1}{C} = \frac{1}{C_{ox}} + \frac{1}{C_H} \approx \frac{d}{rDD_0} = \frac{\Delta d + d_0}{rDD_0} \tag{3}$$

where C_{ox} is the differential capacitance of the oxide film and the measured capacitance (C) is corrected for the roughness factor (r), but not for the Helmoltz double-layer capacitance (C_H), which is assumed to exceed $20\,\mu F\,cm^{-2}$ [8]. D, D_0, Δd and d represent the dielectric constant of the oxide and of the vacuum, the variation in thickness, and the thickness of the initial oxide film, respectively.

The variation in thickness can be calculated from the charge flow, $Q_{tot} = \int i_{ox}\,dt$, assuming that the oxygen evolution (Q_{O_2}), electrolyte decomposition (Q_d), capacitor charging (Q_c) and metal dissolution (Q_{dis}) have negligible contributions (Equation 4) so that the overall charge involved in the anodic process corresponds to the oxide formation (Q_{ox}) (Equation 5). The dissolution-precipitation mechanism of the oxide growth was found to be negligible, but at early stage of a potentiostatic oxide growth [15].

$$Q_{tot} = Q_{ox} + Q_{O_2} + Q_{dis} + Q_d + Q_c \tag{4}$$

$$\Delta d = \frac{Q_{ox} M}{4F\rho r} \tag{5}$$

Here $M = 123.22\,g\,mol^{-1}$, $\rho = 5.89\,g\,cm^{-3}$ for ZrO_2. The roughness factor, r, was assumed to be 2.2 for

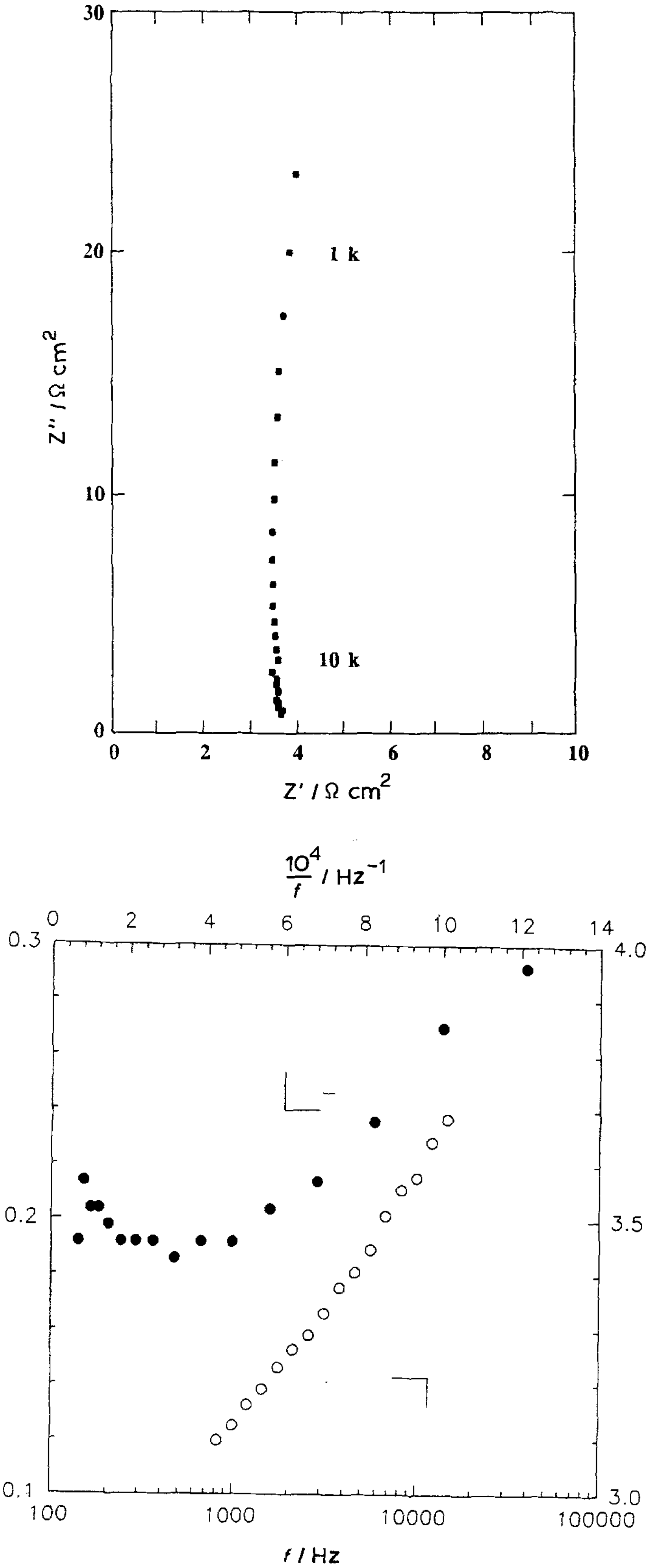

Fig. 1. (a) Impedance plot and (b) Bode plot in the high frequency range for etched zirconium wire at − 1.25 V/SCE in 0.1 M LiOH at 25°C. The mean current density is negligible.

etched zirconium electrodes provided that $r = 1$ for electropolished zirconium [8], even if it was also found to be smoother [6].

The overall charge Q_{tot} and the reciprocal capacitance C^{-1} vary linearly with the electrode potential in the range 0–12 V (Fig. 3), which confirms the negligible contribution of other electrochemical reactions in this range and the linear increase in oxide film thickness with the electrode potential.

A plot of C^{-1} against Δd (Fig. 4) shows a linear dependence, as anticipated from Relation 3 and observed for zirconium in various media [14]. Extrapolation to $C^{-1} = 0$ yields a thickness of 2.0 nm for the initial oxide film, a thin film of a few monolayers, on the

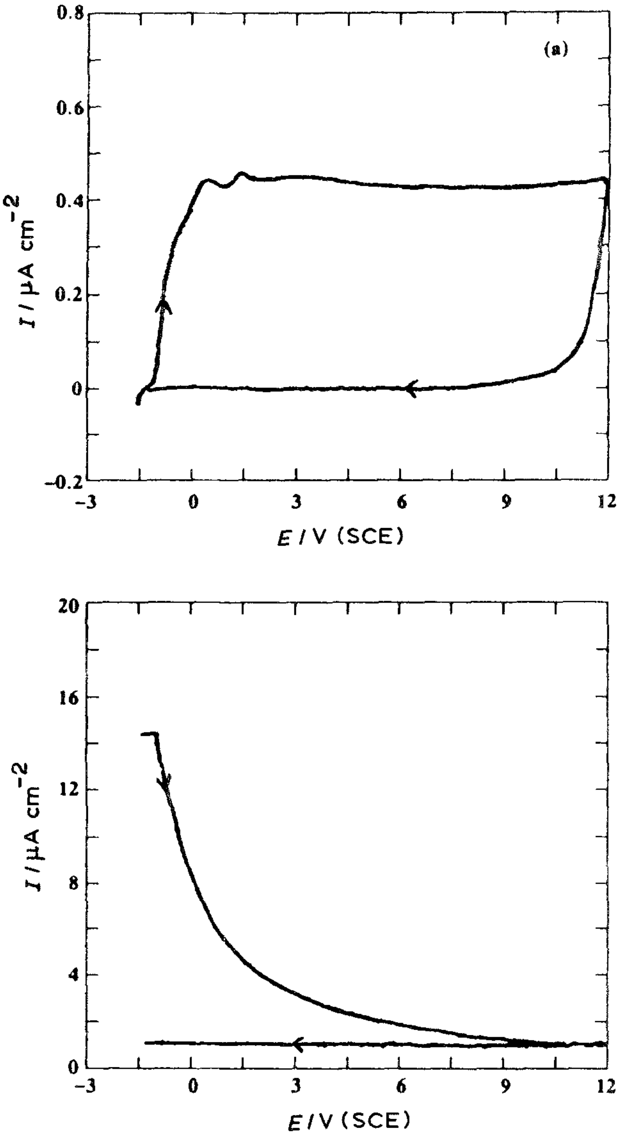

Fig. 2. Potentiodynamic measurements of oxide growth on (a) etched and (b) mechanically polished zirconium wire electrode in 0.1 M LiOH at 25°C. Upper curve: current density; lower curve: electrode capacitance (1 kHz).

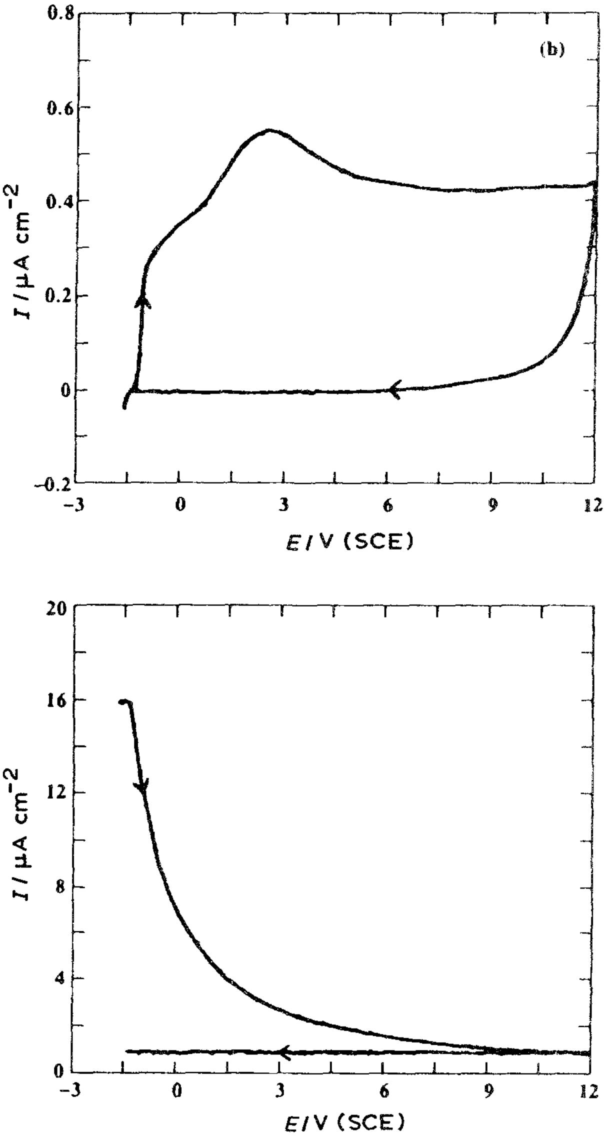

Fig. 2 (*continued*).

etched electrode. An equivalent thickness was reached after 500 s at room temperature in 10^{-8} torr oxygen, after the etching of zirconium [16]. This value is less than the 5 nm reported for the electropolished [8] and etched [14] zirconium and is more or less equivalent to the value reported for etched titanium [13]. The slope of the same plot (Fig. 4) yields a dielectric constant D of $30/r$ which compares well with $28/r$ [10] and 20 [4] determined for the dielectric constant of the oxide film on etched zirconium. It may be pointed out that the D values depends on the estimated surface roughness, the potential sweep rate [13] and the frequency of the measurement, and is therefore difficult to compare with other D values of 20 to 35 [5, 8, 9, 15, 17].

Thus the absolute thickness (d) of the oxide film is a linear function of the formation potential (Fig. 5). The slope of 2.1 nm V^{-1} represents the growth rate of the oxide film in 0.1 M LiOH; this may also be expressed as a field of 0.4 V nm^{-1}. This is similar to 2.5 V^{-1} measured in aqueous ammonium borate solutions [16] and in agreement with the formation rates reported in various other media [4, 17] but slightly different from the values of 2, 6, 3.2 and 3.5 nm V^{-1} obtained for zirconium in acid and alkaline solutions [8]. The growth rate has also been shown to depend on the potential sweep rate [9]. The potential extrapolated to $d = 0$ is -1.5 V, which corresponds approximately to the beginning of the oxide formation. Thus the dielectric constant is not a function of the potential and apparently no incorporation phenomenon occurs in 0.1 M LiOH.

The electronic properties of the oxide film are determined from the C_{ox} against curve for $E < 1.3$ V. At these potentials, the electrode can be expected to behave as an n-type semiconductor and follow the Mott–Shottky equation [18], which can be written for $T = 298$ K as

$$\frac{1}{C_{ox}^2} = \frac{-1.41 \times 10^{20}}{rDN_D}(E_{fb} + 0.026) + \frac{1.41 \times 10^{20}}{rDN_D} \cdot E \tag{6}$$

with C_{ox} in μF cm^{-2} and the potential in volts N_D. V_{fb},

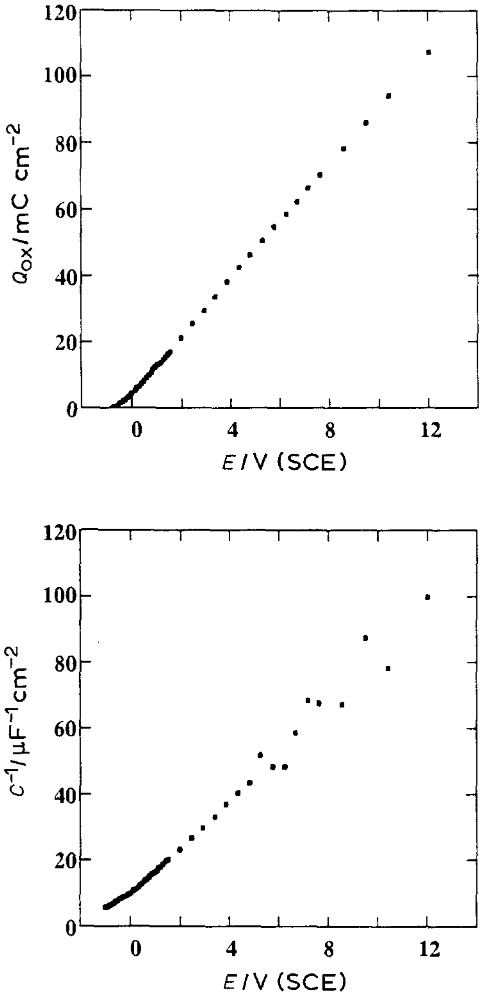

Fig. 3. Dependence of the total anodic charge (Q_{OX}) and the reciprocal capacity (C^{-1}) on the electrode potential for etched zirconium wire electrode in 0.1 M LiOH, 25°C.

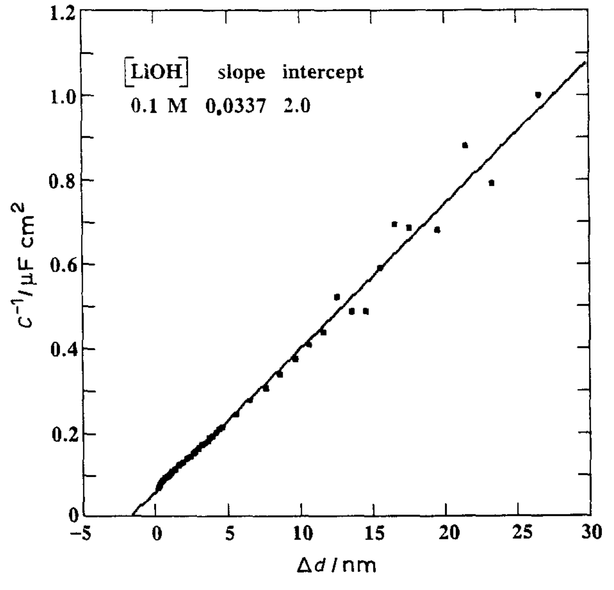

Fig. 4. Dependence of the reciprocal capacity (C^{-1}) on the oxide thickness (Δd) for etched zirconium electrode in 0.1 M LiOH at 25°C. Roughness factor assumed to be equal to 2.2.

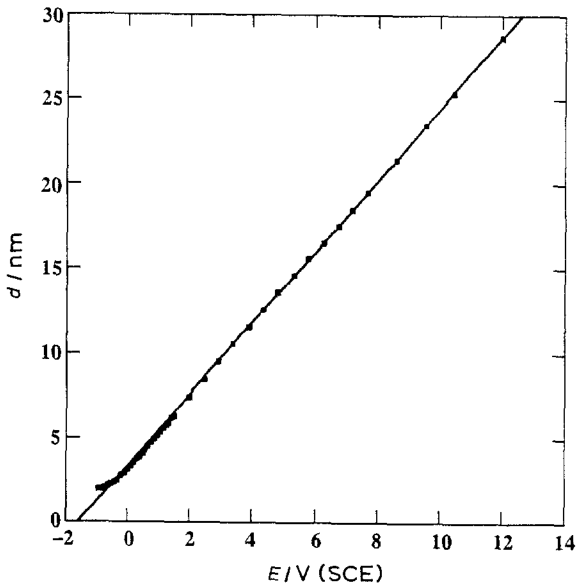

Fig. 5. Dependence of the oxide film thickness on the electrode potential for etched zirconium electrode after potentiodynamic formation of 0.1 M LiOH, 25°C.

r and D are, respectively, the donor density, the flat-band potential, the roughness factor and the dielectric constant of the semiconductor. A plot of C_{ox}^{-2} against E should be linear. The potential where the line intersects the E-axis yields the value of E_{fb} and the slope is used to obtain N_D, since the rD product of the semiconductor oxide film is calculated from the slope of C^{-1} against E plot. A Mott–Schottky analysis at 1000 Hz applied to the residual thin oxide film (Fig. 6) yields $E_{fb} = -1.7$ V SCE and $N_D = 5 \times 10^{20}$ cm^{-3} in 0.1 M LiOH (pH 13). The value for N_D could be compared to $N_D < 3 \times 10^{19}$ cm^{-3} for a 3 V film on zirconium in 0.5 M H_2SO_4 [8] and to $N_D = 1.5 \times 10^{20}$ cm^{-3} for a 1 V TiO_2 film in 0.5 M H_2SO_4 [19], bearing in mind that this parameter is known to decrease with the sweep rate and film thickness [19]. For ZrO_2, the flat-band potential is estimated to be -1.5 V/SCE in 0.5 M H_2SO_4 [8] and -2.0 V/SCE at pH 13 [10, 18].

3.2. *Dissolution of zirconium oxide films*

For a 12 V oxide film formed on zirconium in 0.1 M LiOH, dissolution does not seem to occur in 0.1 M

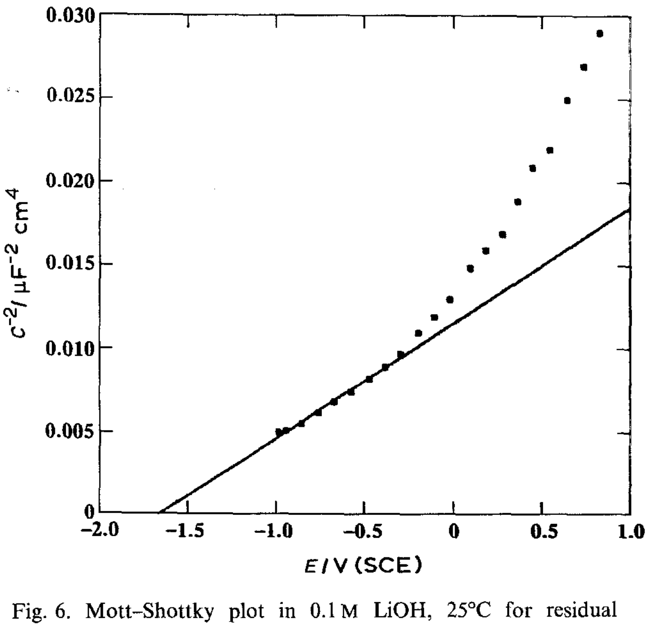

Fig. 6. Mott–Shottky plot in 0.1 M LiOH, 25°C for residual zirconium oxide film after etching.

LiOH, and 1 M HCl because the low capacitance of $0.7\,\mu F\,cm^{-2}$ and the high ohmic resistance remain constant even when recorded for periods of 7 h. The chemical stability agrees with the absence of dissolution below the concentration of 0.5 M NaOH [20] but contrasts with the dissolution process reported in HCl solutions for oxide films formed at a constant current density of $1\,mA\,cm^{-2}$ [11]. In the present case, the open-circuit potential E_{oc} reaches a rest potential of +0.675 V after 200 s in 0.1 M LiOH, whereas it reveals a significant change toward the anodic potential during the first 5000 s in 1 M HCl with a magnitude almost equivalent to that reported in the same medium after 4 h.

The variation of E_{oc} is complex in nature but, generally speaking, a drift toward the negative potential is indicative of oxide film dissolution whereas a drift toward positive potential is indicative of oxide film repair and thickening [21]. A negative shift was reported during the dissolution of TiO_2 in H_2SO_4 and NaOH solutions [22], MoO_2 and ZrO_2 in NaOH solutions [23] but the inverse during the dissolution of ZrO_2 in 1 M HCl [11]. The dissolution rate and the corresponding potential shift were found to depend on the electrolyte concentration [20, 22, 23]. In all cases, the capacitance is assumed to be more sensitive to the dissolution process. This paradoxal behaviour of E_{oc} reflects opposing tendencies and different mechanisms.

A potential drift toward nobler potentials is observed when the 12 V oxide film is immersed in 0.05 M HF. Only the significant increase in capacitance can definitely be attributed to a dissolution process of the oxide film. In 0.05 M HF, the capacitance changes from $0.5\,\mu\,cm^{-2}$ to $\sim 10\,\mu F\,cm^{-2}$, showing a large recovery of the value displayed before the anodization process in 0.1 M LiOH. The similarity of the reciprocal capacitances of oxide films on zirconium in HF and LiOH solutions supports the approximation made in Equation 3 about the negligible comtribution of the Helmholtz double layer.

The observed decrease in the thickness factor (C^{-1}) and the resistance is found to follow an empirical relation in $t^{1/2}$ (Fig. 7). For the thickness:

$$C^{-1} = A - Bt^{1/2} \qquad (7)$$

where A is related to the oxide film thickness at zero immersion time and B to the rate coefficient of the dissolution process [11].

In Fig. 7, only one rate coefficient can be assigned to the dissolution process for films formed at 5.5 and 12 V. The slower decay recorded after the first linear segment does not support the assumption that this oxide film on zirconium is duplex in nature [11, 12]. Indeed, at this point the thickness factor corresponds to a residual film of ~3 nm, whereas the inner layer was found to constitute around 80% of the entire film [24].

Otherwise, the absence of an inflexion point could be due to an equal rate of dissolution for the two hypothetical layers in the more corrosive HF solution, because the specific solid-state nature of each layer would have no effect on the dissolution process. This statement would require more investigation for formation voltages higher than 15 V.

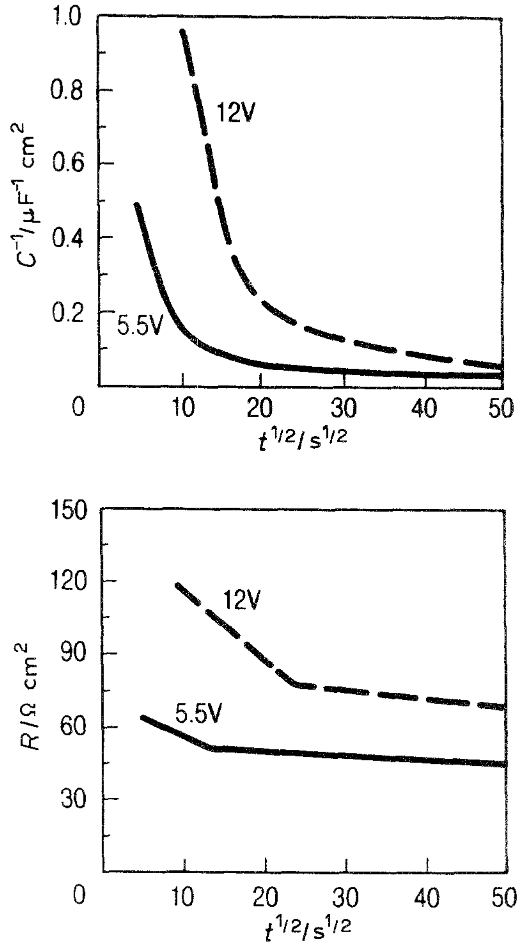

Fig. 7. Reciprocal capacitance and resistance of the 5.5 and 12 V zirconium oxide film as a function of the square root of the immersion time in 0.05 M HF.

As shown in Table 1, the dissolution coefficients in 0.05 M HF reveal that this process in HF solutions is much faster than in 0.5 M H_2SO_4 and 1 M HCl. This result is consistent with the relative dissolution rates of TiO_2 in the same media [25]. The dissolving action of HF solutions appears to be due to the conjugate action of the hydronium and fluoride ions, the latter being ascribed to the formation of fluoride complexes [25]. For formation voltages of 5.5 and 12 V in 0.1 M LiOH, the ratio of their A parameters (see Equation 7) and their dissolution periods is approximately 2, in agreement with the thickness ratio determined from the absolute film thickness against potential curve (Fig. 5). In addition, the dissolution rate (B parameter) increases slightly with the thickness.

For oxide films prepared by heating air at 450°C for 1 min, the dissolution rate of $2\,nm\,s^{-1/2}$ appears to be equivalent to that of oxides prepared in 0.1 M LiOH solution up to 5.5 V (Fig. 8 and Table 1). From the A parameter or the dissolution period, the oxide thickness is estimated to be 200 nm, i.e. in the order of reported values [3]. This suggests that increase of oxide thickness by heating does not increase the defects within the oxide layer, since an increase in the

Table 1. Oxide film dissolution coefficients on Zr *and* Ti *against media and formation conditions*

Metal	*Oxide formation*	*Dissolution medium*	A_1	A_2	B_1	B_2	*Ref.*
			$/cm^2\ \mu F^{-1}$	$/cm^2\ \mu F^{-1}$	$/cm^2\ \mu F^{-1}\ s^{-1/2}$	$/cm^2\ \mu F^{-1}\ s^{-1/2}$	
Zr	10 V, 0.5 M H_2SO_4	1 M HCl	0.47	0.27	6.7	0.77	11
Zr	10 V, 0.5 M H_2SO_4	0.5 M H_2SO_4	0.56	0.52	1.3	0.65	12
Ti	12.5 V, 0.5 M H_2SO_4	0.5 M H_2SO_4	0.26	0.19	1.7	0.72	22
Ti	0.1 M NaOH	0.5 M H_2SO_4	0.27	0.23	0.81	0.22	22
Zr	5.5 V, 0.1 M LiOH	0.05 M HF	0.9	–	82	–	*
Zr	12 V, 0.1 M LiOH	0.05 M HF	2.0	–	100	–	*
Zr	1 min, air 450°C	0.05 M HF	5.8	–	83	–	*

*This work

rate of dissolution was related to the defects within the oxide [20].

4. Conclusion

The anodic growth of ZrO_2 on etched zirconium in 0.1 M LiOH at 25°C yields a 28 nm film at 12 V/SCE which reveals a typical insulating behaviour. Negligible incorporation phenomena seems to occur during anodic growth in lithiated solutions. The chemical dissolution of a film of this thickness is inconsequental in 0.1 M NaOH and 1 M HCl, whereas ZrO_2 rapidly dissolves in 0.05 M HF, at a rate which is almost the same for anodic and thermal films, allowing an estimation of the film thickness.

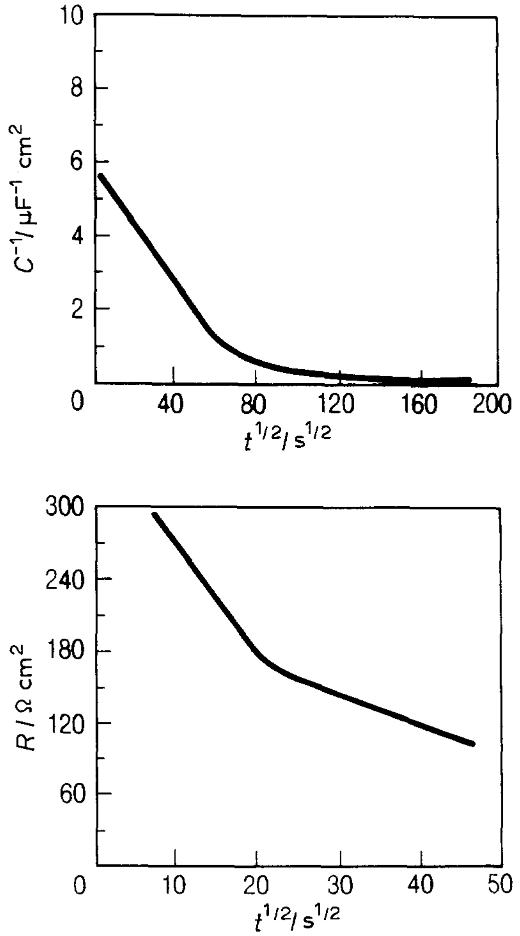

Fig. 8. Reciprocal capacitance and resistance of the zirconium oxide film prepared by heating etched zirconium wire with hot air gun (~450°C) for 1 min as a function of the square root of the immersion time in 0.05 M HF.

Acknowledgments

The author is grateful to Dr J. P. Dodelet of INRS-Energy for fruitful discussions.

References

[1] V. F. Urbanic, *in* 'Zirconium in the Nuclear Industry', (edited by D. G. Franklin and R. B. Adamson), Sixth International Symposium, American Society for Testing and Materials (1984) p. 554.
[2] J. Habeed and D. G. Tuck, *in* 'Encyclopedia of Electrochemistry of the Elements', Vol. IX, (edited by A. J. Bard), Marcel Dekker, New York (1986) Part B, Chap. 3.
[3] M. J. Madou and K. Kinoshita. *Electrochim. Acta* **29** (1984) 411.
[4] B. Cox, *J. Electrochem. Soc.* **117** (1970) 654.
[5] F. DiQuarto, S. Piazza and C. Sunseri, *J. Electrochem. Soc.* **130** (1983) 1014.
[6] J. S. Llewelyn Leach and B. R. Pearson, *Electrochim. Acta* **29** (1984) 1271.
[7] S. Hornkjol, *ibid.* **33** (1988) 289.
[8] P. Meisterjahn, H. W. Hope and J. W. Schultze, *J. Electroanal. Chem.* **217** (1987) 159.
[9] E. M. Patrito, R. M. Torresi, E. P. M. Leiva and V. A. Macagno. *J. Electrochem. Soc.* **137** (1990) 524.
[10] T. Hurten and S. Hornkjol, *Electrochim. Acta* **32** (1987) 811.
[11] M. S. El-Basiouny and A. M. Bekheet, *Br. Corros. J.* **17** (1982) 197.
[12] M. S. El-Basiouny, A. A. Mazhar, F. El-Taib Heakal and M. A. Ameer, *J. Electroanal. Chem.* **147** (1983) 181.
[13] A. G. Gad Allah and A. A. Mazhar, *Corrosion* **46** (1990) 306.
[14] J. A. Bardwell and M. C. H. McKubre, *Electrochim. Acta* **3/4** (1991) 647.
[15] P. Meisterjahn, K. Konig and J. W. Schultze, *ibid.* **34** (1989) 551.
[16] N. Khalil, A. Bowen and J. S. L. Leach, *Electrochim. Acta* **33** (1988) 1721.
[17] C. O. De Gonzalez and E. A. Garcia, *Surf. Sci.* **193** (1988) 305.
[18] S. R. Morrison, 'Electrochemistry at semiconductor and oxidized metal electrodes', Plenum Press, New York (1980) 401 p.
[19] R. M. Torresi, O. M. Camara, C. P. de Pauli and M. C. Giordano, *Electrochim. Acta* **32** (1987) 1291; R. M. Torresi, O. M. Camara and C. P. de Pauli, *ibid.* **32** (1987) 1357.
[20] A. G. Gad-Allan, A. A. Maznar, F. El-Taib Heakal, M. A. Ameer, *J. Appl. Electrochem.* **19** (1989) 213.
[21] A. M. Shams El Din, H. A. El Shayeb and F. M. Abd El Wahab, *J. Electroanal. Chem.* **241** (1986) 567.
[22] M. M. Hefny, A. A. Mazhar and M. S. El-Basiouny, *Br. Corros. J.* **17** (1982) 38.
[23] A. G. Gad-Allah, H. A. Abd El-Rahman, M. M. Abou-Romia, *J. Appl. Electrochem.* **18** (1988) 86.
[24] M. M. Hefny, *J. Appl. Electrochem.* **21** (1991) 483.
[25] L. J. D. Arsov, *Electrochim. Acta* **30** (1985) 1645.